2016

Targeted Imaging of Urothelium Carcinoma in Human Bladders by an ICG pHLIP Peptide Ex vivo

Jovana Golijanin
University of Rhode Island, jgolijanin@uri.edu

Ali Amin

See next page for additional authors

Citation/Publisher Attribution
Golijanin, J., Amin, A., Moshnikova, A., Brito, J. M., Tran, T. Y., Adochite, R., Andreev, G. O.,...Golijanin, D. (2016). Targeted Imaging of Urothelium Carcinoma in Human Bladders by an ICG pHLIP Peptide *Ex vivo*. *Proceedings of the National Academy of Sciences, 113*(42), 11829-11834. doi: 10.1073/pnas.1610472113
Available at: http://doi.org/10.1073/pnas.1610472113

Classification: BIOLOGICAL SCIENCES, Applied Biological Sciences

Targeted imaging of urothelium carcinoma in human bladders by an ICG pHLIP® peptide *Ex vivo*

Jovana Golijanin[1,2], Ali Amin[3], Anna Moshnikova[2], Joseph M. Brito[1], Timothy Y. Tran[1], Ramona-Cosmina Adochite[2], Gregory O. Andreev[2], Troy Crawford[2], Donald M. Engelman[4], Oleg A. Andreev[2], Yana K. Reshetnyak[2], Dragan Golijanin[1]

[1] Minimally Invasive Urology Institute, Division of Urology, The Miriam Hospital and The Warren Alpert Medical School of Brown University, Providence, RI 02906, USA

[2]Physics Department, University of Rhode Island, Kingston, RI 02881

[3] Department of Pathology & Laboratory Medicine, Brown University, The Miriam Hospital, Providence, RI 02906

[4]Department of Molecular Biophysics and Biochemistry, Yale University, New Haven, CT 06511

Keywords: Bladder cancer, fluorescence-guided surgery, NIR imaging, acidity

Corresponding Author: Dragan Golijanin, dgolijanin@lifespan.org

Abstract

Bladder cancer is the fifth most common in incidence and one of the most expensive cancers to treat. Early detection greatly improves the chances of survival and bladder preservation. The pH Low Insertion Peptide (pHLIP® peptide) conjugated with a near infrared fluorescent dye (ICG) targets low extracellular pH allowing visualization of malignant lesions in human bladder carcinoma *ex vivo*. Cystectomy specimens obtained after radical surgery were immediately irrigated with non-buffered saline and instilled with a solution of the ICG pHLIP® construct, incubated, and rinsed. Bladders were subsequently opened and imaged, the fluorescent spots were marked, and a standard pathological analysis was carried out to establish the correlation between ICG pHLIP® imaging and white light pathological assessment. Accurate targeting of bladder lesions was achieved with a sensitivity of 97%. Specificity is 100%, but reduced to 80%, if targeting of necrotic tissue from previous transurethral resections or chemotherapy are considered as false positives. ICG pHLIP® imaging agent marked high grade urothelial carcinomas, both muscle invasive and non-muscle invasive. Carcinoma in situ (CIS) was accurately diagnosed in 11 cases, whereas only 4 cases were seen using white light, so imaging with the ICG pHLIP® peptide offers improved early diagnosis of bladder cancers, and may also enable new treatment alternatives.

Significance Statement

Bladder cancer is the fifth most common cancer. Timely diagnosis and appropriate early management protocols are of paramount significance for improving patient outcomes. This is the first study to show efficient pH dependent near infrared imaging of bladder malignant tumors without targeting of normal tissue. Our results demonstrate that the ICG pHLIP® construct is suitable for use as a predictive clinical marker, specifically staining human bladder tumors after intravesical administration *ex vivo*. The targeting allows delivery of various imaging probes, which may offer early diagnosis and improve the outcomes of endoscopic and radical surgical resection of urothelial carcinomas. In addition; delivery of therapeutic molecules to cancer cells by pHLIP® might open an opportunity for novel targeted treatment of bladder cancers.

\body

Introduction

Bladder cancer is the fifth most common cancer, constituting 4.5% of all new cancer cases in the USA. 76,960 new cases were estimated in 2016 and the death rate currently expected from bladder cancer is 21% (16,390). Approximately 2.4 percent of men and women will be diagnosed with bladder cancer at some point during their lifetime. In 2012, there were an estimated 577,403 individuals living with bladder cancer in the United States. Almost all of these patients require continuous surveillance, and, occasionally, treatments. For all stages combined, the 5-year relative survival rate is 77%. Survival declines to 70% at 10 years and 65% at 15 years after diagnosis. Bladder cancer can be non-muscle or muscle invasive. Half of all bladder cancer patients are diagnosed while the tumor is non-muscle invasive, for which the 5-year survival is 96%. Most (up to 98%) of malignant bladder tumors arise in the epithelium, 90-92% of these bladder cancers are urothelial carcinomas (1, 2). Less common bladder cancers are squamous cell or adenocarcinomas. Approximately 20-25% of patients have muscle invasive disease, and of non-muscle invasive disease patients will progress to muscle invasive disease at 5 years follow up depending on intermediate or high risk of the progression (3, 4). An important medical objective is the identification of early stage lesions, such as carcinoma *in situ*, since it is expected that diagnosis at this stage will decrease the frequency of treatments, increasing patient health and reducing expense.

Each type and stage of bladder cancer requires a different type of treatment. High recurrence frequency, procedural costs, and the requirement for prolonged active monitoring, make bladder cancer one of the most expensive cancers in the US, placing a heavy economic burden on the healthcare system from lifetime endoscopic follow ups and treatments. Patients suffer from high morbidity and the complications associated with chemotherapy, radiation and radical surgery (5). Therefore, as noted, timely diagnosis of the tumor and appropriate management protocols are of great significance for decreasing treatment cost and improving a patient's life style. Advances in the early detection of bladder cancer lesions are likely to increase the

chances of timely successful treatment, the prevention of recurrences, and bladder function preservation.

Cancers, including urothelial carcinoma, are associated with multiple alterations in the genome, including changes in epigenetic regulation, point mutations, gene deletions, duplications and chromosomal rearrangements. These changes are heterogeneous, leading to heterogeneity of the overexpression of particular biomarkers at the surfaces of cancer cells within a tumor and between tumors. Heterogeneity significantly limits success in the use of cell surface biomarkers for the targeted delivery of therapeutics. On other hand, multiple studies have revealed that neoplastic cells produce an acidic environment due to increased metabolic activity (6). Adaptations to the highly acidic microenvironment are critical steps in the transition from an avascular pre-invasive tumor to a malignant invasive carcinoma (7-9). Thus, acidity may provide a universal biomarker for tumor targeting that is not subject to the selection of resistant cell lines (10). pH Low Insertion Peptides (pHLIP® peptides) are a class of membrane-binding peptides that specifically target acidic cells *in vitro* and *in vivo* (11) by inserting across cellular membranes when the extracellular pH is low (12). pHLIP® peptides conjugated with fluorescent dyes have been used to differentiate normal from neoplastic tissue in various animal tumor models (12-15), and in human biopsy head and neck samples (16, 17). This report is the first study using an ICG pHLIP® conjugate for the diagnosis of urothelial carcinoma and precancerous lesions in fresh human radical cystectomy samples *ex vivo*, and points the way toward a wide range of diagnostic and therapeutic alternatives.

Results

We used a pHLIP® peptide labeled with a near-infrared fluorescence (NIRF) dye, ICG, to monitor the targeting of tumors in human bladders. The absorption spectrum of ICG pHLIP® is shown in Figure 1a. The fluorescence of ICG pHLIP® increases about 25 fold in the presence of 1-palmitoyl-2-oleoyl-sn-glycero-3-phosphocholine (POPC) liposomes (Figure 1b). Thus, binding of ICG pHLIP® to the lipid bilayers of cancerous cell membranes significantly enhances the emission of ICG.

From November 2014 through December 2015, twenty two radical cystectomy patients were included in the study. Patient ages ranged from 51 to 84 (mean age 67.7 years), and the gender ratio: M/F was 19/3. Table 1 contains patient demographics, preoperative diagnosis, clinical stage of the disease and the results of imaging studies. The specimens did not show any adverse morphological findings after incubation with ICG pHLIP®, and there was no evidence of damage or degenerative effect in the non-tumoral tissue. The use of ICG pHLIP® did not alter the pathological assessment of the radical cystectomy tissues. Overall, 29 malignant lesions were identified by pathology assessment of the 22 bladder specimens stained with ICG pHLIP® (3 radical cystectomy cases were incubated *ex vivo* with ICG-Cys as negative controls). The frequencies of different pathologies in 29 lesions were as follows (Figure 2): high grade muscle invasive urothelial carcinoma (HGI) in 12; high grade non-muscle invasive urothelial carcinoma (HGN) in 5; carcinoma in situ (CIS) in 11, and high grade dysplasia in 1. In 7 cases NIRF imaging guided the pathologist to CIS not observed by white light inspection. In case #2 necrotic tissue inside a diverticulum was NIRF positive. For the negative control cases (cases #13, 19 and 20) only the ICG-Cys dye alone was used for instillation (at concentrations from 8 to 40 μM in an 80 ml volume), and no specific tumor targeting was observed.

The tabular results of the sensitivity/specificity tests are shown in Tables 2-3. The test was performed for cancerous versus normal tissue excluding targeting of necrotic and previously treated tissue (Tables 2a and 2b). The sensitivity and specificity of targeting of cancerous tissue versus normal were found to be 97% and 100%, respectively. If targeting of necrotic tissue from prior post trans-urethral removal of bladder tumors and previously treated (chemotherapy) necrotic tumors by ICG pHLIP® is considered as a false positive, the specificity is reduced from 100% to 80% (Tables 3a and 3b).

Discussion

We used an ICG pHLIP® construct to target urothelial carcinoma in human bladder specimens immediately after surgical removal. ICG is an FDA approved NIRF dye that does not show any

independent propensity for targeting neoplastic tissue as seen in renal cell carcinoma, mostly by perfusion and diffusion differences or neoplastic and normal tissue (washout). ICG is in clinical use to visualize vasculature or lymphatics (18-20). ICG has a low level of fluorescence in aqueous solution, while its emission increases upon binding to hydrophobic pockets of proteins (such as albumin) or cellular membranes. Targeting by the pHLIP® peptide is based on low pH-triggered insertion into the lipid bilayers of cancer cell membranes. Thus, the pHLIP® peptide tethers the ICG to the membrane, enhancing ICG fluorescence by about 25 fold.

To avoid/minimize targeting of normal cells by the ICG pHLIP® peptide, the construct was instilled in pH 7.4 PBS supplemented with 10 mM of D-glucose. to promote the uptake of the ICG pHLIP® peptide by cancer cells. Glycolytic cancer cells exhibit high glucose uptake, which enhances acidification of the extracellular space *in vitro* and *in vivo* (21). Thus, our goal was to selectively promote increased acidity at cancer cell surfaces to enhance pHLIP® peptide insertion and targeting, while not affecting normal cells with normal metabolism.

In our study we had a mixture of different subtypes of urothelial carcinoma, as expected given that the disease had advanced to the point where the bladder had to be removed. Our cases included typical high grade urothelial carcinoma but also had different variants with prominent squamous cell differentiation, micropapillary urothelial carcinoma, adenocarcinoma and plasmacytoid morphology. It appears that the sensitivity (97%) and specificity (100%) of tumor targeting by ICG pHLIP® peptide is irrelevant to the subtype of tumor. Half of the cystectomy specimens in our study revealed evidence of necrosis and effects from prior treatments, and all revealed evidence of residual tumor (invasive or in-situ) adjacent and associated with necrosis, which was targeted by ICG pHLIP® peptide, possibly from entrapment or uptake of ICG by necrotic areas. Our previous studies did not show targeting of necrotic tissue by pHLIP® peptides in animal tumor models (14). If targeting of necrotic and previously treated tissues are considered as false positives, the specificity is decreased to 80%, but no false positives were seen for unperturbed lesions.

One lesion gave a positive NIRF imaging signal in the presence of dysplasia, revealed by subsequent pathology analysis. Urothelial dysplasia is an incidental microscopic finding where urothelial cells show mild atypical features short of the diagnosis of carcinoma in situ. It is considered a pre-cancerous process and studies have shown that up to 19% of urothelial dysplasia cases develop urothelial carcinoma (22-24). Although precancerous, it is recommended that patients with dysplasia receive proper clinical follow up for early detection of an imminent carcinoma. Dysplasia has not been clinically detectable, so the ICG pHLIP® peptide may be a useful marker for detection of high grade dysplasia in urothelium, allowing early detection of precancerous lesions.

Bladder tissues are prone to inflammation and infection. Long standing inflammation and severe infections can cause transformations in the mucosa like cystitis cystica and cystitis glandularis that, due to high frequency, are considered normal findings in the urothelium. In one case, an area with marked uptake of ICG pHLIP® peptide showed cystitis cystica et glandularis with chronic inflammation without any evidence of dysplasia or malignancy. It is noteworthy that almost all 22 cystectomy specimens revealed some degree of cystitis cystica et glandularis somewhere in the specimen. Only two lesions revealed cystitis cystica without any other pathology: one lesion (case #9) showed positive signal with ICG pHLIP® peptide. When the instilled concentration of ICG pHLIP® peptide was reduced to 4 µM, the cystitis cystica in the second case (case #18) was not stained. Reducing the concentration of ICG pHLIP® peptide did not affect targeting of high grade invasive carcinoma and CIS (case #17). We expect that optimizing the concentration and shortening the time of the ICG pHLIP® instillation will allow a clear signal differentiation among inflamed, necrotic and cancerous tissue.

In summary, the ICG pHLIP® peptide is a promising tool for the early detection of urothelial carcinoma, regardless of subtype, with high sensitivity and specificity. The detection might be used for monitoring the state of disease and/or for marking lesions for surgical removal. Before ICG pHLIP® imaging agent enters clinical trial the toxicology and pharmacology studies will be

carried out to establish safety profile. The ICG pHLIP® imaging agent is expected to improve diagnosis and resection of cancerous lesions in the bladder. As a result, the recurrence rate might be reduced, patient outcomes could be improved and the cost of medical care for bladder cancer will be lowered. In addition, success with targeted imaging could lead to pHLIP® delivery of therapeutic molecules to bladder tumor cells, creating an opportunity for targeted treatment of bladder cancers. Currently, we are testing novel pHLIP® based therapeutic agents, which demonstrate very promising results. Further, the ICG pHLIP® construct is a generally applicable imaging agent, since it targets a general property of the tumor microenvironment, tumor acidity. Once approved for clinical use, it could be tested and possibly used on a variety of cancers. We have shown targeting of primary tumors and metastatic lesions by fluorescent pHLIP® peptides in more than 15 varieties of human, murine and rat tumors, including lymphoma, melanoma, pancreatic, breast and prostate transgenic mouse models and human tissue (bladder, kidney, breast and head/neck stained *ex vivo*).

Materials and Methods

Conjugation of ICG with the pHLIP® peptide

pHLIP® variant 3 (Var3) peptide with a single Cys residue at the N-terminus, ACDDQNPWRAYLDLLFPTDTLLLDLLWA, was synthesized and purified by reversed phase chromatography by CS Bio, Inc. The near infrared fluorescent dye, indocyanine green (ICG) maleimide (Intrace Medical), was conjugated to the pHLIP® peptide at a ratio of 1:1 in DMF (dimethylformamide). The reaction progress was monitored by the reversed phase (Zorbax SB-C18 columns, 9.4 × 250 mm 5 µm, Agilent Technology) high-performance liquid chromatography (HPLC) using a gradient from 5-70% acetonitrile in water containing 0.05% trifluoroacetic acid. Also, for the negative control, ICG-malemide was conjugated with the free amino aicd, L-cysteine (Sigma). The concentration of labeled peptide in buffer was determined by ICG absorption at 800 nm, ε_{800}=137,000 M^{-1} cm^{-1}. The purity of the constructs was performed by analytical HPLC and SELDI-TOF mass spectrometry, the amount of free dye in the solution was less than 1%.

Liposome Preparation

Large unilamellar vesicles were prepared by extrusion. 2.5 mg POPC (1-palmitoyl-2-oleoyl-snglycero-3-phosphocholine, Avanti Polar Lipids, Inc.) lipids were dissolved in 0.5 ml chloroform, desolvated on a rotary evaporator and dried under high vacuum for 3 hours. The phospholipid film was then rehydrated in pH 7.4 PBS containing 10 mM D-glucose, vortexed for 5 minutes, and repeatedly extruded at least 15 times through a membrane with a 100 nm pore size.

Absorption and Fluorescence Measurements

Absorbance and fluorescence measurements were carried out on a Genesys 10S UV-Vis spectrophotometer (Thermo Scientific) and a SpectraMax M2 spectrofluorometer (Molecular Devices), respectively. The absorption spectra were measured in PBS pH 7.4 containing 10 mM D-glucose from 600 to 850 nm. The fluorescence spectra of 10 μM of ICG pHLIP® peptide were measured from 810 to 850 nm at 790 nm excitation wavelength in PBS pH 7.4 containing 10 mM D-glucose, with or without 2 mM of POPC liposomes.

***Ex vivo* Imaging of Bladder Specimens**

After obtaining institutional review board (IRB) approval, 22 urothelial carcinoma patients that were scheduled for radical cystectomy were selected over a twelve month period and appropriate informed consent was obtained. After radical cystectomy, bladder specimens were immediately removed and irrigated 3 times for 5 min via catheter with non-buffered saline and instilled and incubated with 80 ml of 8 μM or 32.8 μg/ml (unless otherwise is stated, see notes to Table 1) of ICG pHLIP® construct or ICG-Cys in PBS pH 7.4 containing 10 mM D-glucose for 60 minutes. Then, the unbound constructs were removed by rinsing with 80 ml of saline solution 3-5 times, the bladder was irrigated thoroughly with buffered saline and opened using a Y incision on the anterior wall. Using a da Vinci Si NIRF imaging system (Firefly^{R}), *ex vivo* fluorescent and white light imaging of the entire bladder and its parts was performed. The

fluorescent spots were marked and standard pathological analysis was carried out to explore the correlation between appearance of fluorescent signal and cancer lesions.

Pathological Analysis

The specimen was sectioned and submitted after 24 hour fixation in 10% phosphate-buffered formalin according to the standard institutional grossing manual, with emphasis on the marked areas of the bladder. The sections were processed for routine histology into paraffin-embedded blocks. Five micrometer thick tissue sections were obtained and stained for hematoxylin and eosin (H&E). Evaluation of pathology was performed by a genitourinary (GU) pathologist, and a standard report was prepared based on the American Joint Committee on Cancer (AJCC) Cancer Staging Manual, 7th edition, 2010.

Statistical Analysis

Statistical parameters were calculated according to the following equations:

$$TRP = \frac{TP}{TP+FN}; \quad SPC = \frac{TN}{TN+FP}$$

$$PPV = \frac{TP}{TP+FP}; \quad NPV = \frac{TN}{FN+TN};$$

$$FPR = \frac{FP}{FP+TN}; \quad FNR = \frac{FN}{TP+FN};$$

$$FDR = \frac{FP}{TP+FP}; \quad FOR = \frac{FN}{FP+TN}$$

Where *TP* is the true positive; *TN* is the true negative; *FP* is the false positive; *FN* is the false negative; *TRP* is the true positive rate or sensitivity; *SPC* is the true negative rate or specificity; *PPV* is the positive predictive value or precision; *NPV* is the negative predictive values; *FPR* is the false positive rate; *FNR* is the false negative rate; *FDR* is the false discovery rate; *FOR* is the false omission rate.

Acknowledgements

This work was supported by NIH grant GM073857 to DME, OAA and YKR.

Conflict statement

DME, OAA, and YKR have founded and have a financial interest in a company, pHLIP, Inc., with the aim of bringing pHLIP technology to the clinic. The company has had no involvement in funding the studies reported here.

Author contributions

D Golijanin, A Amin, OA Andreev and YK Reshetnyak designed research; J Golijanin, A Amin, A Moshnikova, J Brito, T Tran, R-C Adochite, T Crawford and D Golijanin performed research; J Golijanin, D. Golijanin, A Amin, GO Andreev, OA Andreev and YK Reshetnyak analyzed data; A Amin, DM Engelman, OA Andreev, YK Reshetnyak and D Golijanin wrote the paper.

References

1. Siegel R, Naishadham D, & Jemal A (2012) Cancer statistics, 2012. *CA Cancer J Clin* 62(1):10-29.
2. Pasin E, Josephson DY, Mitra AP, Cote RJ, & Stein JP (2008) Superficial bladder cancer: an update on etiology, molecular development, classification, and natural history. *Rev Urol* 10(1):31-43.
3. Anastasiadis A & de Reijke TM (2012) Best practice in the treatment of nonmuscle invasive bladder cancer. *Ther Adv Urol* 4(1):13-32.
4. Kamat AM*, et al.* (2014) Defining and treating the spectrum of intermediate risk nonmuscle invasive bladder cancer. *J Urol* 192(2):305-315.
5. Mariotto AB, Yabroff KR, Shao Y, Feuer EJ, & Brown ML (2011) Projections of the cost of cancer care in the United States: 2010-2020. *J Natl Cancer Inst* 103(2):117-128.
6. Damaghi M, Wojtkowiak JW, & Gillies RJ (2013) pH sensing and regulation in cancer. *Front Physiol* 4:370.
7. Gillies RJ, Verduzco D, & Gatenby RA (2012) Evolutionary dynamics of carcinogenesis and why targeted therapy does not work. *Nat Rev Cancer* 12(7):487-493.
8. Estrella V*, et al.* (2013) Acidity generated by the tumor microenvironment drives local invasion. *Cancer Res* 73(5):1524-1535.
9. Gatenby RA, Gawlinski ET, Gmitro AF, Kaylor B, & Gillies RJ (2006) Acid-mediated tumor invasion: a multidisciplinary study. *Cancer Res* 66(10):5216-5223.
10. Bailey KM, Wojtkowiak JW, Hashim AI, & Gillies RJ (2012) Targeting the metabolic microenvironment of tumors. *Adv Pharmacol* 65:63-107.
11. Andreev OA, Engelman DM, & Reshetnyak YK (2014) Targeting diseased tissues by pHLIP insertion at low cell surface pH. *Front Physiol* 5:97.
12. Weerakkody D*, et al.* (2013) Family of pH (low) insertion peptides for tumor targeting. *Proc Natl Acad Sci U S A* 110(15):5834-5839.
13. Reshetnyak YK*, et al.* (2011) Measuring tumor aggressiveness and targeting metastatic lesions with fluorescent pHLIP. *Mol Imaging Biol* 13(6):1146-1156.

14. Adochite RC*, et al.* (2014) Targeting breast tumors with pH (low) insertion peptides. *Mol Pharm* 11(8):2896-2905.
15. Cruz-Monserrate Z*, et al.* (2014) Targeting pancreatic ductal adenocarcinoma acidic microenvironment. *Sci Rep* 4:4410.
16. Luo Z*, et al.* (2014) Widefield optical imaging of changes in uptake of glucose and tissue extracellular pH in head and neck cancer. *Cancer Prev Res (Phila)* 7(10):1035-1044.
17. Luo Z, Tikekar RV, Samadzadeh KM, & Nitin N (2012) Optical molecular imaging approach for rapid assessment of response of individual cancer cells to chemotherapy. *J Biomed Opt* 17(10):106006.
18. Tobis S*, et al.* (2012) Robot-assisted and laparoscopic partial nephrectomy with near infrared fluorescence imaging. *J Endourol* 26(7):797-802.
19. Alander JT*, et al.* (2012) A review of indocyanine green fluorescent imaging in surgery. *Int J Biomed Imaging* 2012:940585.
20. Desmettre T, Devoisselle JM, & Mordon S (2000) Fluorescence properties and metabolic features of indocyanine green (ICG) as related to angiography. *Surv Ophthalmol* 45(1):15-27.
21. Kozin SV, Shkarin P, & Gerweck LE (2001) The cell transmembrane pH gradient in tumors enhances cytotoxicity of specific weak acid chemotherapeutics. *Cancer Res* 61(12):4740-4743.
22. Althausen AF, Prout GR, Jr., & Daly JJ (1976) Non-invasive papillary carcinoma of the bladder associated with carcinoma in situ. *J Urol* 116(5):575-580.
23. Smith G*, et al.* (1983) Prognostic significance of biopsy results of normal-looking mucosa in cases of superficial bladder cancer. *Br J Urol* 55(6):665-669.
24. Zuk RJ, Rogers HS, Martin JE, & Baithun SI (1988) Clinicopathological importance of primary dysplasia of bladder. *J Clin Pathol* 41(12):1277-1280.

Table 1. Demographic information, pathological stage and diagnosis, lesions seen by white light and fluorescence imaging.

Case #	Sex Age	Pathological stage	Pathological diagnosis	Grade	Lesion number	White light diagnosis	Fluor.
1	M/63	pT3aN1	Infiltrating high grade urothelial carcinoma, CIS & necrosis	HGI	1	+	+
2	M/61	pT0N0	Diverticulum with urothelial atypia & treatment effects	-	-	+	+
3	F/84	ypT3bN0	Invasive high grade urothelial carcinoma Invasive high grade urothelial carcinoma & necrosis	HGI HGI	2 3	+ +	+ +
4	M/51	pT2aN1	Residual infiltrative high grade urothelial carcinoma micropapillary features, dysplasia & necrosis	HGI	4	+	+
5	M/69	pTaN0	Non-invasive high grade papillary carcinoma	HGN	5	+	+
6	M/65	pT1N0	Residual invasive high grade urothelial carcinoma, CIS & necrosis CIS CIS	HGI CIS CIS	6 7 8	+ + +	+ + +
7	M/61	pT1N0	Focally invasive high grade urothelial carcinoma, necrosis	HGI	9	+	+
8	M/79	pT1N0	Dysplasia Treatment effect & CCCG	DIS -	10 -	- -	+ +
9	M/74	pT0N0	CCCG	-	-	-	+
10	F/82	pT1N0	Non-invasive high grade urothelial carcinoma Invasive high grade urothelial carcinoma CIS CIS & CCCG	HGN HGI CIS CIS	11 12 13 14	+ + - -	+ - + +
11	M/68	pTisN0	CIS & CCCG CIS	CIS CIS	15 16	+ -	+ +
12	M/71	pTisN0	Non-invasive high grade urothelial carcinoma Non-invasive high grade urothelial carcinoma CIS CIS	HGN HGN CIS CIS	17 18 19 20	+ + - -	+ + + +
13*	M/66	pT3N1	Invasive high grade urothelial carcinoma Ulceration, necrosis, CCCG			+ +	ICG-Cys
14	M/66	pT1N0	Non-invasive high grade urothelial carcinoma	HGN	21	+	+
15	M/57	pT1N0	Invasive high grade urothelial carcinoma	HGI	22	+	+
16	F/77	pTisN0	CIS with early invasion CIS with early invasion	CIS CIS	23 24	+ -	+ +
17**	M/57	pT1bN0	Invasive high grade urothelial carcinoma CIS with early invasion Necrosis & treatment effect	HGI CIS -	25 26 -	+ + +	+ + +
18**	M/72	pT3aN0	Invasive high grade urothelial carcinoma, CIS Necrosis & treatment effect in diverticulum	HGI -	27 -	+ +	+ -
19	M/64	pT2aN0	Invasive high grade urothelial carcinoma, CIS, Necrosis & treatment effect			+	ICG-Cys
20	M/63	ypT0N0	CCCG and reactive changes in scar			+	ICG-Cys
21	M/74	pT3aN0	Invasive high grade urothelial carcinoma in scar Necrosis	HGI -	28 -	+ +	+ +
22**	M/66	ypT3aN0	Invasive high grade urothelial carcinoma with neuroendocrine features	HGI	29	+	+

* 40 µM of 80 mL of the construct was used for instillation

** 4 µM of 80 mL of the construct was used for instillation

Table 2a. Tabular results of the sensitivity/specificity test of ICG pHLIP® peptide targeting of cancerous lesions in the human bladder specimens: Carcinoma versus Normal excluding necrotic tissue and treatment effects.

Receiver operator characteristics carcinoma vs normal	*TP* + *FN*	*FP* + *TN*	Sum
TP + *FP*	*TP*, 28	*FP*, 0	28
FN + *TN*	*FN*, 1	*TN*, 19	20
Sum	29	19	

TP is the true positive; *TN* is the true negative; *FP* is the false positive; *FN* is the false negative

Table 2b. Descriptive parameters

Measure	Results
Sensitivity, *TRP*	0.966
Specificity, *SPC*	1.000
Positive predictive value, *PPV*	1.000
Negative predictive values, *NPV*	0.950
False positive rate, *FPR*	0.000
False negative rate, *FNR*	0.034
False discovery rate, *FDR*	0.000
False omission rate, *FOR*	0.053

Table 3a. Tabular results of the sensitivity/specificity test of ICG pHLIP® peptide targeting of cancerous lesions in the human bladder specimens: Carcinoma versus Normal including necrotic tissue and treatment effects.

Receiver operator characteristics carcinoma vs normal + necrosis	*TP* + *FN*	*FP* + *TN*	Sum
TP + *FP*	*TP*, 28	*FP*, 5	33
FN + *TN*	*FN*, 1	*TN*, 20	21
Sum	29	25	

TP is the true positive; *TN* is the true negative; *FP* is the false positive; *FN* is the false negative

Table 3b. Descriptive parameters

Measure	Results
Sensitivity, *TRP*	0.966
Specificity, *SPC*	0.800
Positive predictive value, *PPV*	0.848
Negative predictive values, *NPV*	0.952
False positive rate, *FPR*	0.020
False negative rate, *FNR*	0.034
False discovery rate, *FDR*	0.152
False omission rate, *FOR*	0.040

Figures Legends

Figure 1. Normalized absorbance (***a***) and fluorescence (***b***) spectra are shown of ICG pHLIP® construct measured in PBS pH 7.4 containing 10 mM D-glucose. The fluorescence (with an excitation wavelength of 790 nm) of ICG pHLIP® construct is increased about 25 fold in the presence of POPC liposomes compared to the emission in buffer.

Figure 2. Representative white light (***a***, ***d, g, j***), NIR fluorescence (***b***, ***e, h, k***) *ex vivo* imaging of bladder specimens and hemolysin and eosin (HE) stained tumor sections (***c***, ***f, i, l***) are shown, demonstrating targeting of invasive high grade urothelial carcinoma (***a***, ***b***, ***c***), non-invasive high grade urothelial carcinoma (***d, e, f***), carcinoma in situ (***g, h, i***) and dysplasia (***j, k, l***) by ICG pHLIP® imaging agent. The diagnosis was confirmed by pathological analysis. The fluorescent lesions were marked in case #11 to identify locations for pathology analysis.

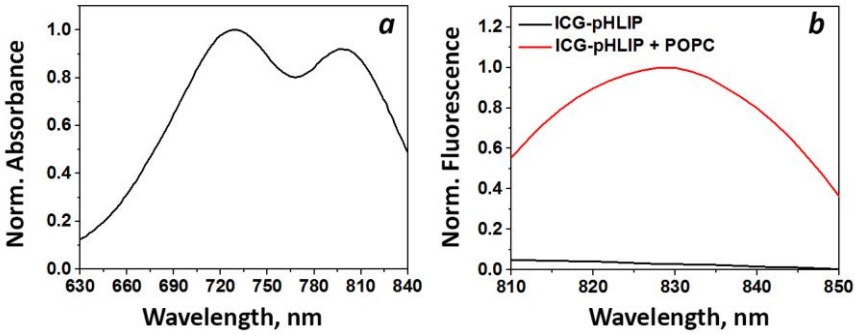
a
Norm. Absorbance
1.0
0.8
0.6
0.4
0.2
0.0
630 660 690 720 750 780 810 840
Wavelength, nm
b
ICG-pHLIP
ICG-pHLIP + POPC
Norm. Fluorescence
1.2
1.0
0.8
0.6
0.4
0.2
0.0
810 820 830 840 850
Wavelength, nm

Figure 1

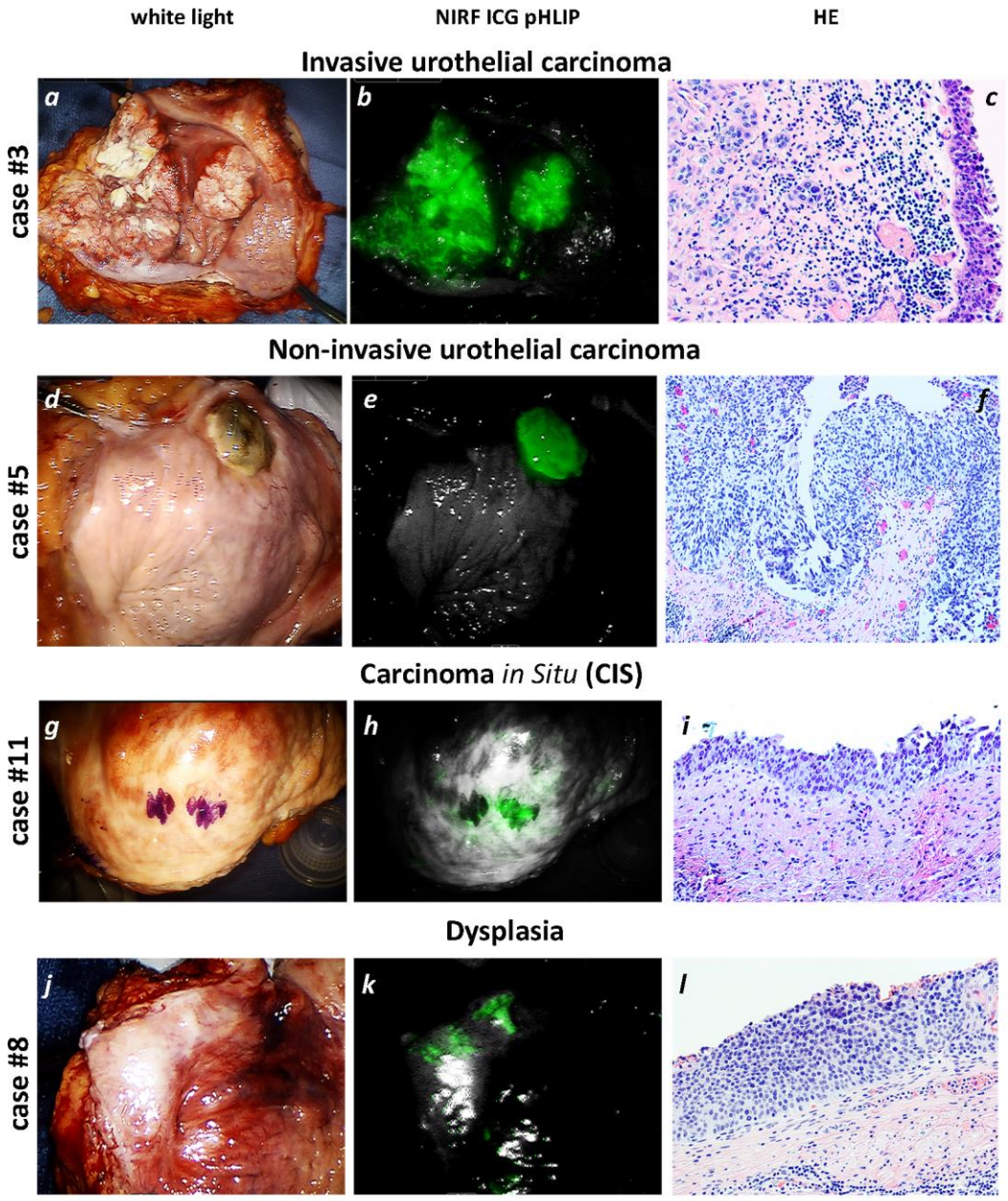
white light
NIRF ICG pHLIP
HE
Invasive urothelial carcinoma
case #3
a
b
c
Non-invasive urothelial carcinoma
case #5
d
e
f
Carcinoma in Situ (CIS)
case #11
g
h
i
Dysplasia
case #8
j
k
l

Figure 2